Molecular Simulation Studies of the Orientation and Conformation of Cytochrome c Adsorbed on Self-Assembled Monolayers

Jian Zhou, Jie Zheng, and Shaoyi Jiang*

Department of Chemical Engineering, University of Washington, Seattle, Washington 98195

Received: December 30, 2003; In Final Form: April 27, 2004

Cytochrome *c* (Cyt-c) is an important membrane electron-transfer protein. To maximize its electron transfer, adsorbed Cyt-c should have a preferred orientation with its heme ring close and perpendicular to the surface. Moreover, the adsorbed Cyt-c should keep its native conformation. In this work, the orientation and conformation of Cyt-c adsorbed on carboxyl-terminated self-assembled monolayers (SAMs) are investigated by a combined Monte Carlo and molecular dynamics simulation approach. The root-mean-square deviation, radius of gyration, eccentricity, dipole moment, heme orientation, and superimposed structures of Cyt-c were calculated. Simulation results show that the desired orientation of Cyt-c with its heme group perpendicular to the surface could be obtained on a negatively charged surface. The direction of the dipole of Cyt-c, contributed significantly by both lysine residues near the surface and glutamic acid residues far away from the surface, determines the final orientation of Cyt-c adsorbed on a charged surface. Lysine residues Lys25, Lys27, Lys72, and Lys79 are responsible for the strong electrostatic interactions with the surface. A possible electron-transfer pathway is proposed (i.e., iron−His18−Cys17−Gln16−surface and iron−Met80−Lys79−surface). The effect of the strength of negatively charged surfaces on the conformation of adsorbed Cyt-c is studied. Although higher surface charge density of a negatively charged surface favors its preferred orientation, too high a surface charge density will cause a severe conformational change of the adsorbed protein, resulting in the loss of bioactivity of the adsorbed protein.

Introduction

Cytochrome c (Cyt-c), a membrane electron-transfer (ET) protein, plays an important role not only in a wide range of basic biological processes but also in many applications such as protein chromatography, drug delivery on solid substrates, biosensors, biofuel cells, bioelectronic devices, and so forth.[1−20] For these processes and applications, one key issue is the orientation of the adsorbed Cyt-c on surfaces. To enable fast ET, adsorbed Cyt-c should have an orientation with the heme ring close and perpendicular to surfaces. Another key issue that determines the activity of the adsorbed protein is its conformation (i.e., how the conformation of the adsorbed protein resembles that of its native state).

For experimental studies of Cyt-c orientation, Saavedra and co-workers[21−27] determined the orientation distribution of the porphyrin groups in adsorbed Cyt-c films using a combination of two techniques (i.e., absorbance linear dichroism measured in planar integrated optical waveguide-attenuated total reflection (IOW-ATR) geometry and fluorescence anisotropy measured in total internal reflection fluorescence (TIRF) geometry). The orientation of Cyt-c on surfaces was also studied by surface-enhanced resonance Raman scattering (SERRS),[11] polarized X-ray absorption fine structure (XAFS) spectroscopy,[28] and an electrochemistry method.[14] It is generally thought that the desired orientation could be obtained on negatively charged surfaces,[6−8] which is possibly because of the lysine patch of Cyt-c.[10,12,20]

It has been widely believed that proteins undergo some conformational change when adsorbed on surfaces. Soft proteins are susceptible to conformational changes when adsorbed on solid surfaces.[29,30] To investigate the conformational change of adsorbed proteins, Burkett et al.[31] performed circular dichroism (CD) spectroscopy and ^{1}H NMR spectroscopy studies of the adsorbed α-helical peptide and found a partial loss in its helicity upon adsorption. However, the CD technique cannot directly provide specific information about which regions of the molecule interact with the surface. Highly sensitive differential scanning calorimetry (DSC),[30] Fourier transform infrared-attenuated total reflection (FTIR-ATR),[32] sum frequency generation (SFG) vibrational spectroscopy,[33] time-of-flight secondary ion mass spectrometry (TOF-SIMS),[34] second harmonic generation-circular dichroism (SHG-CD),[35] and electrochemistry[14,36] approaches were also used to study protein conformational changes on surfaces. It has been observed that proteins adsorbed on hydrophobic surfaces generally undergo structural rearrangement such that nonpolar amino acids interact preferentially with the surfaces, which gives rise to strong interfacial interactions and irreversible adsorption.

Molecular simulations are well suited to studying protein adsorption behavior on surfaces and provide molecular-level information. Molecular simulations of proteins at interfaces can be carried out at three levels (i.e., colloid-bead, united-residue, and all-atom models). The simplest one is based on a colloid model in which the protein is modeled as a charged sphere[37,38] or as a combination of charged spheres.[39] For the residue model, each amino acid residue is represented by an interaction site. We developed a generalized residue model to predict the orientation of IgG1 and IgG2a on charged surfaces,[40] and the prediction was verified by our surface plasmon resonance (SPR)[41] and TOF-SIMS experiments.[42] Simulation studies of

* To whom correspondence should be addressed. E-mail: sjiang@u.washington.edu.

10.1021/jp038048x CCC: $27.50
Published on Web 08/07/2004

protein adsorption based on all-atom models were performed using Monte Carlo (MC)[39,43] and Brownian dynamics (BD)[44] simulation methods with the solvent described as a continuous dielectric media. Tobias et al.[45] performed molecular dynamics (MD) simulations to study the behavior of yeast Cyt-c on surfaces in vacuum. Cyt-c was covalently tethered to hydrophobic (methyl-terminated) and hydrophilic (thiol-terminated) self-assembled monolayers (SAM) by disulfide linkage with its unique cysteine residue. They found that on the hydrophobic SAM surface the protein is oriented so that the heme plane is more nearly parallel to the surface whereas on the hydrophilic SAM surface it is more nearly perpendicular. Nordgren et al.[46] extended the work by Tobias et al.[45] to simulations of a hydrated protein on surfaces. However, only water layers near the protein and surface (~500 water molecules) were considered. In their work,[45,46] because the Cyt-c was chemically linked to the surface with the unique cysteine residue, the orientation of Cyt-c was largely predetermined. Castells et al.[47] performed MC simulations to study the conformational change of lattice-model proteins adsorbed on a solid surface. Properties of Cyt-c in solutions have been studied using MD simulations.[48−50] Besides molecular simulations, protein adsorption was also studied theoretically. Lenhoff and co-workers[51−55] systematically investigated protein−surface interaction energies by solving the Poisson−Boltzmann equation in both atomistic and colloidal frameworks. They found that negative adsorption free energy was dominated by a very small fraction of the configurations and that electrostatic interactions were very important. Szleifer and co-workers[56,57] studied the kinetics and thermodynamics of protein adsorption by a generalized molecular theoretical approach.

SAMs are ideal platforms for the study of protein adsorption.[58−62] Besides, biological interfaces could be mimicked by electrodes coated with SAMs. Bowden and co-workers pioneered the study of the adsorption and electrochemistry of Cyt-c on carboxyl-terminated SAMs.[6−8] The interactions between the protein and the surface have a large impact on the orientation and conformation of adsorbed proteins and therefore on their biological activity. However, the electrochemical behavior of Cyt-c at the electrode/solution interface is still far from being completely understood. It is generally believed that the lysine patches[10,12,20] may have an influence on the orientation of Cyt-c on negatively charged surfaces, but there is a lack of direct evidence. So far, the ET pathway is not clear. Feduro[4] pointed out that the degree of ionization of surface-attached acid groups was expected to affect the strength of Cyt-c binding to the electrode surface as well as the thermodynamics and kinetics of interfacial ET reactions associated with Cyt-c. Chen et al.[14] chose SAMs terminating in the SO_3^- group as a charged surface in their experiments, which should have a higher surface charge density than COOH SAMs. They found that no redox peaks were observed for Cyt-c adsorbed on the sulfonate SAM, although their SPR studies indicated that the SAM adsorbed approximately a double layer of Cyt-c.[14] To investigate the mechanism of Cyt-c orientation and to find suitable surfaces for the rational control of the orientation and conformation of adsorbed Cyt-c, in this work, we use the Monte Carlo method to obtain the orientation of Cyt-c on SAM surfaces first. Then, using MD simulations, we further research the subsequent conformational change of adsorbed protein on SAM surfaces with different surface charge densities.

Simulation Details

Cyt-c consists of 104 residues and 1 heme ring. The high-resolution crystal structure of horse heart Cyt-c (pdb code: 1hrc), refined to 1.9 Å by Bushnell et al.,[63] served as the starting point of the simulation. Hydrogen atoms were added by the CHARMM package.[64] For the all-atom structure of Cyt-c, there are a total of 1744 atoms. The protein was simulated at pH 7.0. The N terminus of Cyt-c was acetylated. The arginine (Arg) and lysine (Lys) residues were taken to be protonated, whereas glutamic acid (Glu) and aspartic acid (Asp) residues along with the C terminus were taken to be deprotonated. Histidine (His) adopts the neutral protonation state (HSD) in this work. For the Fe−S bond,[65] the bond length used is 2.32 Å, and the force constant is 65.0 kcal·mol^{-1}·Å^{-2}. The protein has a net charge of +6e. Only one protein molecule was considered in the simulations. The potential parameters for Cyt-c are from the CHARMM force field for proteins.[64]

For the surface, the $\sqrt{3} \times \sqrt{3}$ structure of $HS(CH_2)_9COOH$ SAMs on Au(111) was adopted, which consist of 168 thiol chains and 1512 gold atoms. For thiol chains in the studied systems, 8, 42, or 84 chains are deprotonated, representing a degree of dissociation of 5, 25, or 50% for negatively charged SAMs, respectively. Chen et al.[14] chose SAMs terminating in the SO_3^- group as a charged surface in their experiments, which should have a higher surface charge density than COOH SAMs. For simplicity, we used COO− SAMs with different degrees of dissociation to represent various negatively charged surfaces. The surface has dimensions of 59.94 Å × 60.4 Å. The potential parameters for SAMs are from the CHARMM force field for lipids.[66]

The temperature of the simulated system was 300 K. For MC simulations, initially the center of mass of the protein was put 5 nm above the surface with a random orientation. During simulations, the protein was kept rigid. It was translated and rotated around its center of mass. The displacement of each move was adjusted to ensure an acceptance ratio of 0.5. One million configurations were sampled. With the preliminarily optimized orientation of Cyt-c on SAM surfaces from MC simulations, water molecules were added to a simulated box of 59.94 Å × 60.4 Å × 61.0 Å. The added water molecules were selected such that no water oxygen atom was closer than 2.8 Å to the protein and surfaces. There are 4160 water molecules in the system, which are described by the TIP3P model.[67] To keep the system neutral, we added 6 chlorine ions to the simulated box and 8, 42, and 84 sodium ions for carboxyl-SAM surfaces with degrees of dissociation of 5, 25, and 50%, respectively. The ions are modeled by a potential proposed by Beglov and Roux.[68] Each simulation system has a total of 21 622 atoms. With the CHARMM27b4 package, the system was minimized in 200 cycles by using the steepest descent method, with the protein atoms being kept fixed. The whole system was heated to 300 K and preequilibrated for 1000 steps. The protein was still constrained at its crystal structure during this stage. Then, the preequilibrated configuration of the whole system was loaded into our MD simulations. The initial velocity of each atom was assigned from a Maxwell−Boltzmann distribution at 300 K. The Berendsen method[69] was used to keep the temperature of the system constant. The system was coupled with a heat bath, using a coupling time of 0.1 ps. The gold atoms and the sulfur atoms of SAMs were kept fixed during the simulations. Bonds containing hydrogen were kept rigid using the RATTLE[70] method with a geometric tolerance of 10^{-6}. A cell-linked list[71] was employed to accelerate the simulation. The short-range nonbonded interactions were calculated by a switched potential with a switching function starting at 10 Å and reaching zero at a distance of 11 Å. Electrostatic interactions were calculated by the shifted potential with a cutoff distance of 11 Å. Two-

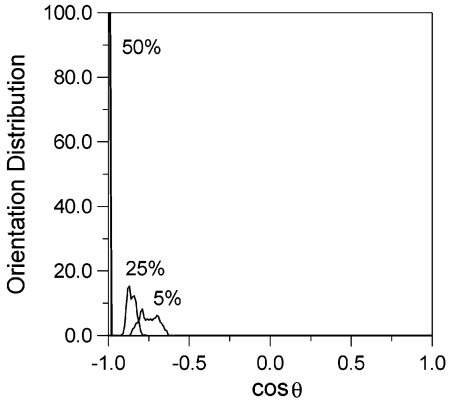

Figure 1. Orientation distribution of Cyt-c adsorbed on carboxyl-terminated SAMs.

TABLE 1: Averaged Properties of Cyt-c by MD Simulations

	orientation	heme angle	R_{gyr} (Å)	eccentricity	rmsd (Å)	dipole (D)
crystal			12.64	0.144		255
bulk			12.88	0.143	1.60	279
5%	−0.75	81	12.96	0.151	1.71	271
25%	−0.86	93	13.03	0.145	1.97	364
50%	−0.99	109	13.05	0.138	2.64	661

dimensional periodic boundary conditions were used in the simulations. There is a hard wall on the top of the simulation box, and a reflective boundary condition is applied. Each MD simulation was carried out over a period of 1 ns with a time step of 1 fs.

Results and Discussion

The orientation and conformation of Cyt-c on negatively charged carboxyl-SAMs with different degrees of dissociation of 5, 25, and 50% were investigated by a combined MC and MD simulation approach. For comparison, Cyt-c behavior in the bulk solution was also studied. The preliminary orientation of Cyt-c on SAM surfaces was obtained from MC simulations. The optimal orientation, radius of gyration, eccentricity, root-mean-square deviation (rmsd), superimposed structures, and dipole moment of Cyt-c were calculated during the MD simulations. Simulation results are summarized in Table 1 and Figures1−7. In Table 1, the reported results were averaged over 500 ps after equilibration.

Orientation. The orientation angle is used to quantitatively characterize the orientation of Cyt-c on different surfaces. The orientation angle of the adsorbed Cyt-c molecule is defined as the angle between the unit vector normal to the surface and the unit vector along the dipole of Cyt-c. The cosine value of this angle is used to represent the orientation of adsorbed Cyt-c. The orientation distributions of Cyt-c on SAM surfaces are shown in Figure 1. The heme tilt angle is defined as the angle between the unit vector normal to the surface and the unit vector normal to the heme plane. From Table 1 and Figure 1, it can be seen that there is a preferred orientation for Cyt-c on each negatively charged surface. The larger the surface charge density, the closer to −1.0 the cosine of the orientation angle and the narrower the orientation distribution. The direction of the dipole of Cyt-c is more antiparallel to the unit vector normal to the surface; this also indicates that the electrostatic interactions dominate for negatively charged surfaces investigated in this work. The dipole moment of Cyt-c is an important factor in determining the orientation of Cyt-c on negatively charged surfaces. This charge-driven mechanism of protein orientation is consistent with the finding in our previous works[39,40] for the study of antibody orientation by using colloid, residue, and all-atom models.

Figure 2a−c displays the final Cyt-c configurations by MD simulations on carboxyl-terminated SAMs with degrees of dissociation of (a) 5, (b) 25, and (c) 50%. For these negatively charged surfaces, a more strongly charged surface forms more COO^-/NH_3^+ salt bridges with Cyt-c and provides stronger electronic coupling with the protein. It is obvious that more side chains of lysine residues are directed toward the surface for the SAM with a 50% degree of dissociation (Figure 2c) than for SAMs with a 5 or 25% degree of dissociation (Figure 2a and b). Du et al.[27] obtained a significantly narrower orientation distribution of Cyt-c on sulfonate-terminated SAMs than distributions measured previously on other types of SAMs. The experimental observation[27] is consistent with our molecular simulation results because sulfonate-terminated SAMs have a higher surface charge density than carboxyl-terminated SAMs.[14]

Table 1 and Figure 2a−c show that the heme group is almost perpendicular to the surface. The desired orientation is obtained on carboxyl-terminated negatively charged SAMs. It has long been believed that the lysine residues contribute mostly to the final orientation and that this cluster of basic residues facilitates their adsorption to acidic surfaces. As mentioned by Fedurco,[4] there exist as many as 18 lysine residues distributed rather homogeneously around the heme on the protein surface. As shown in Figure 2a−c, the lysine residues (blue) are distributed over the entire protein, not only around the heme. With an analysis of negatively charged residues, we find that all eight glutamic acid residues (red) are far away from the surface. As mentioned by Burkett et al.,[31] a few small patches of a large and complicated protein may determine the overall conformation, orientation, and activity of the adsorbed protein. Here, we find that this part of the glutamic acid residues contributes significantly to the dipole of the protein and results in the final orientation of the adsorbed Cyt-c as shown in Figure 2.

Binding Sites and Electron-Transport Pathway. From the preferred orientation of Cyt-c on carboxyl-terminated SAMs with a 5% degree of dissociation, we further analyze the residues close to the surface. They are displayed in Figure 3 with the same orientation as that in Figure 2a. For lysine residues, Lys25, Lys27, Lys72, and Lys79 are responsible for the strong electrostatic interactions with the surface. This finding clarifies the specific lysine residues that contribute most to the interaction with negatively charged surfaces. The residues, such as Gln16, Thr28, Thr47, and Ile81, provide van der Waals interactions with the surface.

The preferred orientation of Cyt-c with respect to the surface shown in Figure 2 would allow for fast electron transfer. From the simulation-predicted preferred orientation, we propose a possible electron-transport pathway, shown in Figure 4. The redox center consists of heme iron, complexed by four nitrogen atoms of the porphyrin ring, and two amino acids, histidine (His18) and methionine (Met80), serve as axial ligands. From Figure 4, it is clear that the heme edge is very close to the surface. Cyt-c with Lys79 and Gln16 residues is directed toward the surface. Thus, the possible ET pathway is iron−His18−Cys17−Gln16−surface and iron−Met80−Lys79−surface. Fedurco previously proposed two possible electron-transport pathways in his review paper.[4] Our simulation results support pathway B of his assumptions.

rmsd and Superimposed Structures. The root-mean-square deviation (rmsd) is defined as rmsd $= \sqrt{\langle \sum_{i=1}^{N} m_i (r_a - r_{a,ref})^2 \rangle / \sum_{i=1}^{N} m_i}$, where N is the number of protein

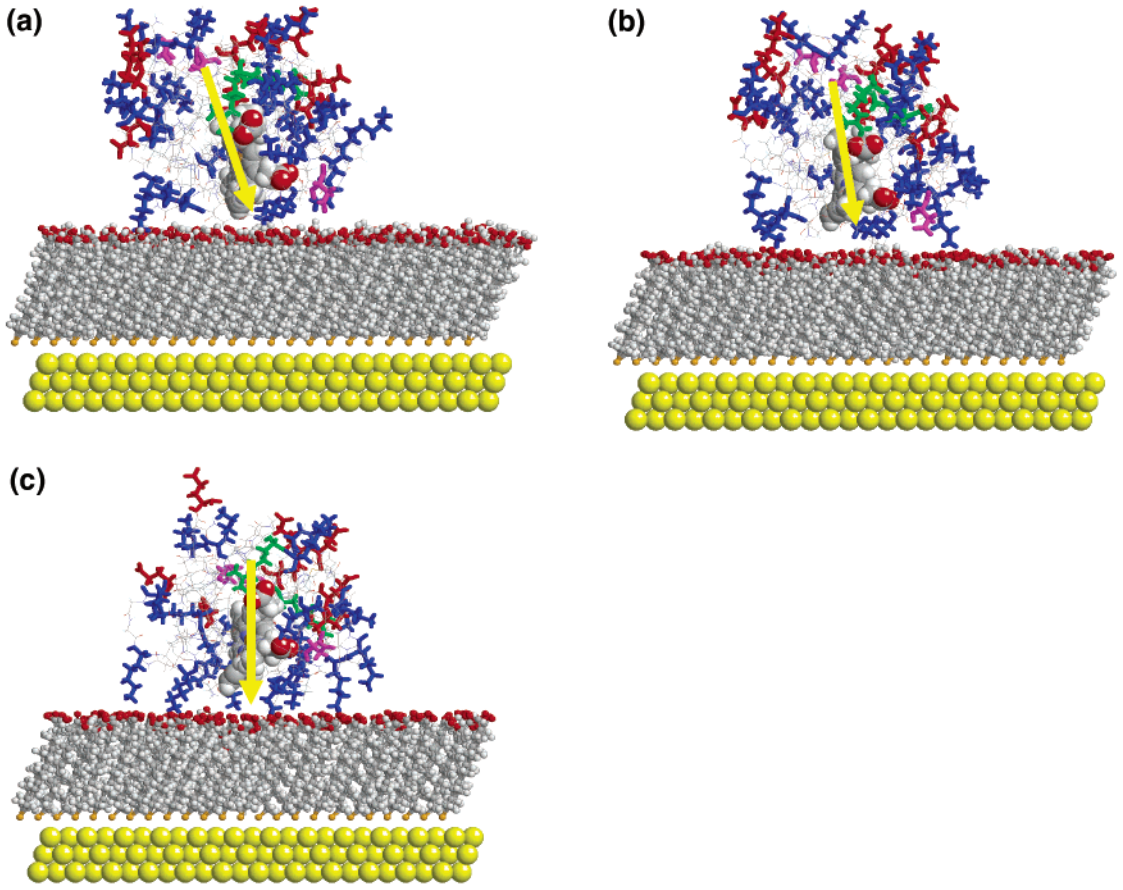

Figure 2. Cyt-c configurations on carboxyl-terminated SAMs with degrees of dissociation of (a) 5, (b) 25, and (c) 50%. For clarity, water molecules and ions are not shown. The yellow space-filled representation is for gold; the ball-stick representation is for SAM; the CPK space-filling representation is for heme; the stick representation is for charged residues Lys (blue), Arg (green), Glu (red), and Asp (magenta); and the wire-frame representation is for other residues in Cyt-c. The yellow arrow indicates the direction of the dipole of Cyt-c.

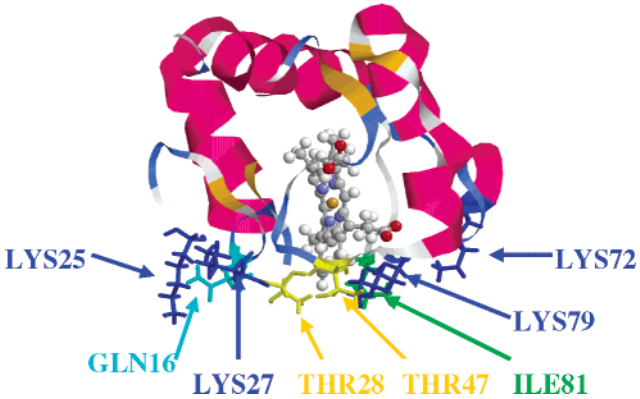

Figure 3. Residues of Cyt-c near the SAM surface with a 5% degree of dissociation.

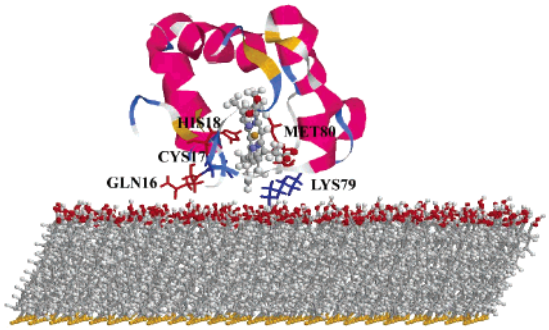

Figure 4. Simulation-predicted electron-transfer pathway of Cyt-c on negatively charged surfaces.

atoms. It represents the minimum root-mean-square deviation between one simulated structure and its reference structure. In this work, the crystal structure of Cyt-c was used as the reference structure. The evolution of the rmsd as a function of time for Cyt-c in bulk solution and on SAM surfaces is shown in Figure 5. The simulated structures of Cyt-c on surfaces and in bulk solution were superimposed on its crystal structure by the molecular graphical program VMD.[72] They are shown in Figure 6. This provides a visual assessment of the overall structure of the protein in solution and on surfaces. From Table 1 and Figure 5, it can be seen that the rmsd value of the bulk solution is 1.60 Å and is comparable to that of tuna Cyt-c in water by Wong et al.[48] (i.e., 1.71 Å). From Figure 6a, it can be seen that most of the features of the secondary structure were preserved to a large extent for the structure in bulk solution compared with its crystal structure. As found in work by Stocker at al.,[73] the behavior of a protein in solution is very similar to that in its crystal environment. For the structures of Cyt-c on SAM surfaces with degrees of dissociation of 5, 25, and 50%, the rmsd values are 1.71, 1.97, and 2.64 Å, respectively. They are 6.9, 23, and 65% larger, respectively, than that in bulk solution. Thus, a larger conformational change is observed on a charged surface with a higher surface charge density. A charged surface with too high a surface charge density may cause a severe conformational change and the denaturation of adsorbed proteins, leading to the loss of its bioactivity. Chen et al.[14] found that no redox peaks were observed for Cyt-c adsorbed on sulfonate SAM. Because the SO_3^--terminated SAM is strongly charged, the interactions between the SAM surface and the

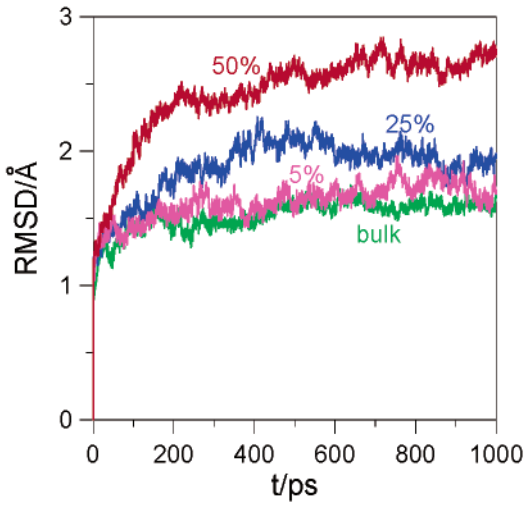

Figure 5. rmsd as a function of time for Cyt-c in bulk solution and on SAM surfaces.

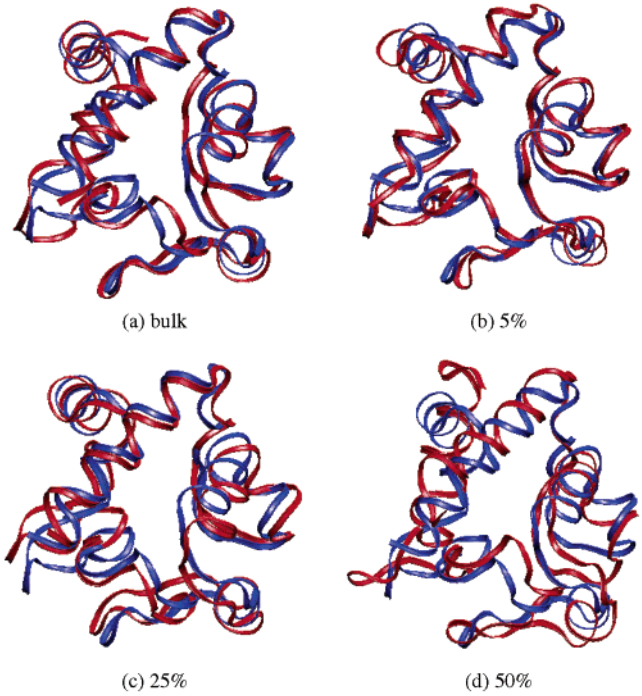

Figure 6. Simulated structure of Cyt-c (red) (a) in bulk solution and on SAM surfaces with degrees of dissociation of (b) 5, (c) 25, and (d) 50% superimposed on the crystal structure of Cyt-c (blue).

protein are also strong. However, interactions that are too strong may cause a much larger conformational change in the adsorbed protein and result in the denaturation of adsorbed Cyt-c. This is possibly why there are no redox peaks observed for Cyt-c adsorbed on sulfonate SAMs. In Figure 6b, for the 5% case, almost all of the secondary structure of Cyt-c is retained. This surface could be compared with the hydrophilic surfaces by Tobias et al.[45] and Nordgren et al.[46] because the degree of dissociation is not high and electrostatic interactions are not very strong. Tobias et al.[45] found that the secondary structure of adsorbed Cyt-c, dominated by α helices, was not significantly affected. Nordgren et al.[46] also found that the overall protein structure was largely conserved, except at each end of the sequence and in one loop region. With the increase in surface charge density, the structure of adsorbed Cyt-c is more distorted as shown in Figure 6c and d. In terms of the rmsd, the structure of the 5% case is closer to that of Cyt-c in bulk solution than to that of the 50% case, which shows that the Cyt-c structure on this surface more closely resembles that of the native state; therefore, this surface could be used to immobilize Cyt-c for practical applications because both the desired orientation and native conformation are acquired on this surface. In previous studies, Tobias et al.[45] obtained rmsd values of 3.2 and 2.9 Å for yeast Cyt-c on hydrophobic and hydrophilic surfaces in vacuum, respectively. Because of the screened protein−SAM interactions in water solutions, the rmsd values of fully hydrated Cyt-c are smaller compared with their results. Nordgren et al.[46] observed the dependence of rmsd values on the number of water molecules and thought that more water molecules help to maintain protein structure in simulations more akin to its crystal structure.

Radius of Gyration and Eccentricity. The radius of gyration of a protein, R_g, is defined as $R_g = \sqrt{1/M(\Sigma_{i=1}^{N} m_i(r_i - r_{COM})^2)}$, where M and r_{COM} are the molecular weight and the center of mass of the protein; m_i and r_i are the mass and position of each atom, respectively. It represents a mass-weighted root-mean-square average distance of all atoms in a protein from its center of mass, which could characterize the overall size of a protein. From Table 1, it can be seen that the radius of gyration of Cyt-c is 12.88 Å when solvated in bulk solution and 12.96, 13.03, and 13.05 Å when adsorbed on SAM surfaces. They are 1.9, 2.5, 3.1, and 3.2% larger, respectively, than that of its crystal structure, 12.64 Å. The radii of gyration of Cyt-c on surfaces are 0.62, 1.16, and 1.32% larger when compared with that in bulk solution. Nordgren et al.[46] also observed an increase of gyration radius when Cyt-c was adsorbed on surfaces. The gyration radius of Cyt-c solvated in bulk solution, 12.88 Å (simulated in this work), is almost equal to that in dense solution, 12.88 Å, or that in sparse solution, 12.89 Å, as determined by Nordgren et al.[46]

The eccentricity of a protein is another parameter that could be used to characterize the overall shape of a protein. It is defined as $1 - I_{ave}/I_{max}$, in which I_{max} is the maximal principal moment of inertia and I_{ave} is the average of three principal moments of inertia. From Table 1, it can be seen that for the 50% case, eccentricity is much smaller than for other cases. Because the long axis of the ellipsoidal protein is parallel to the surface and the protein stretches in the direction normal to the surface, Cyt-c looks more globular. For other cases, the values of the eccentricity are close to each other.

Dipole. The dipole is defined as $\vec{\mu} = \sum_{i=1}^{N} q_i(r_i - r_{COM})$, where q_i is the partial charge of each atom and r_{COM} is the position of the center of mass of the protein. The evolution of the dipole moment as a function of time for Cyt-c in bulk solution and on SAM surfaces is displayed in Figure 7. As shown in Table 1 and Figure 7, the dipole moments of Cyt-c in bulk solution and on the 5% surface are slightly larger than that in its crystal state. The dipole moment (279 D) of Cyt-c in bulk solution is very close to that (271 D) of Cyt-c on the 5% dissociated carboxyl-terminated SAM. The dipole moments of Cyt-c on more strongly charged SAM surfaces with degrees of dissociation of 25 and 50% are 1.3 and 2.4 times larger, respectively, than that in bulk solution. The much larger dipole moments are due to the larger structural change induced by more strongly charged surfaces because of the stronger attraction between the positive lysine residues and the negatively charged surface and the repulsion between the negative glutamic acid residues and the negatively charged surface. The importance of the dipole moment and its change was seldom addressed in previous simulation studies of protein adsorption. The dipole moment of Cyt-c on the 50% surface is much larger than that

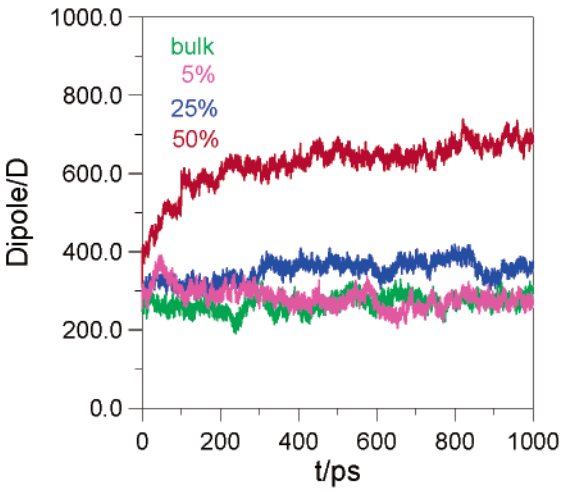

Figure 7. Dipole moment as a function of time for Cyt-c in bulk solution and on SAM surfaces.

of Cyt-c on other surfaces. Although a larger dipole moment and a stronger charged surface favor a narrower protein orientation distribution, a much larger protein conformational change from its native structure on this surface may cause the loss of bioactivity of adsorbed Cyt-c. As pointed out by Fedurco,[4] long-range electrostatic forces, acting at the polarized electrochemical interface, can bring this highly charged metalloprotein into the adsorbed state, in which protein unfolding and spin-state changes on the heme iron might occur. From this work and other experiments,[14] the conformational change of adsorbed Cyt-c on a strongly dissociated, negatively charged surface would be too large. The native state conformation cannot be conserved, which is not favorable for practical applications.

Conclusions

In this work, the orientation and conformation of Cyt-c on carboxyl-terminated SAMs are investigated by a combined Monte Carlo and molecular dynamics simulation approach. Cyt-c adsorbed on carboxyl-terminated SAMs could achieve the desired orientation in which the heme group is perpendicular to the surface. The direction of the dipole of Cyt-c, contributed significantly by the lysine residues near the surface, and glutamic acid residues far away from the surface, determines the final orientation of adsorbed Cyt-c. Lysine residues Lys25, Lys27, Lys72, and Lys79 are responsible for strong electrostatic interactions with surfaces. On the basis of simulation results, a possible ET pathway is proposed (i.e., iron−His18−Cys17−Gln16−surface and iron−Met80−Lys79−surface. Though strongly charged surfaces lead to the preferred orientation with a narrower distribution, they will cause a larger conformational change and the loss of bioactivity of adsorbed protein. People should pay attention to the strength of a charged surface to ensure both the desired orientation and native conformation. This work sheds light on the mechanism of the orientation and conformation of adsorbed proteins at the molecular level and provides useful information for the design and development of biosensors and other bioelectronic devices.

Acknowledgment. We acknowledge the Defense Advanced Research Projects Agency (F30602-01-2-0542) for financial support.

References and Notes

(1) Herron, J. N.; Wang, H. K.; Janatova, V.; Durtschi, J. D.; Caldwell, K. D.; Christensen, D. A.; Chang, I. N.; Huang, S. C. In *Biopolymers at Interfaces*; Marcel Dekker: New York, 1998, p 221.
(2) Jeuken, L. J. C. *Biochim. Biophys. Acta-Bioenergetics* **2003**, *1604*, 67.
(3) Davis, J. J.; Hill, H. A. O.; Bond, A. M. *Chem. Rev.* **2000**, *200*, 411.
(4) Fedurco, M. *Coord. Chem. Rev.* **2000**, *209*, 263.
(5) Zhang, J.; Chi, Q.; Kuznetsov, A. M.; Hansen, A. G.; Wackerbarth, H.; Christensen, H. E. M.; Andersen, J. E. T.; Ulstrup, J. *J. Phys. Chem. B* **2002**, *106*, 1131.
(6) Tarlov, M. J.; Bowden, E. F. *J. Am. Chem. Soc.* **1991**, *113*, 1847.
(7) Collinson, M.; Bowden, E. F.; Tarlov, M. J. *Langmuir* **1992**, *8*, 1247.
(8) Song, S.; Clark, R. A.; Bowden, E. F.; Tarlov, M. J. *J. Phys. Chem.* **1993**, *97*, 6564.
(9) Leopold, M. C.; Bowden, E. F. *Langmuir* **2002**, *18*, 2239.
(10) Kuznetsov, B. A.; Byzova, N. A.; Shumakovich, G. P. *J. Electroanal. Chem.* **1994**, *371*, 85.
(11) Macdonald, I. D. G.; Smith, W. E. *Langmuir* **1996**, *12*, 706.
(12) Avila, A.; Gregory, B. W.; Niki, K.; Cotton, T. M. *J. Phys. Chem. B* **2000**, *104*, 2579.
(13) Dick, L. A.; Haes, A. J.; Van Duyne, R. P. *J. Phys. Chem. B* **2000**, *104*, 11752.
(14) Chen, X. X.; Ferrigno, R.; Yang, J.; Whitesides G. M. *Langmuir* **2002**, *18*, 7009.
(15) Hobara, D.; Imabayashi, S.; Kakiuchi, T. *Nano Lett.* **2002**, *2*, 1021.
(16) Wei, J. J.; Liu, H. Y.; Khoshtariya, D. E.; Yamamoto, H.; Dick, A.; Waldeck, D. H. *Angew. Chem., Int. Ed.* **2002**, *41*, 4700.
(17) Wei, J. J.; Liu, H. Y.; Dick, A.; Yamamoto, H.; He, Y. F.; Waldeck, D. H. *J. Am. Chem. Soc.* **2002**, *124*, 9591.
(18) Khoshtariya, D. E.; Wei, J. J.; Liu, H. Y.; Yue, H. J.; Waldeck, D. H. *J. Am. Chem. Soc.* **2003**, *125*, 7704.
(19) Liu, H. Y.; Yamamoto, H. Wei, J. J.; Waldeck, D. H. *Langmuir* **2003**, *19*, 2378.
(20) Xu, W. S.; Zhou, H.; Regnier, F. E. *Anal. Chem.* **2003**, *75*, 1931.
(21) Edmiston, P. L.; Wood, L. L.; Lee, J. E.; Saavedra, S. S. *J. Phys. Chem.* **1996**, *100*, 775.
(22) Lee, J. E.; Saavedra, S. S. *Langmuir* **1996**, *12*, 4025.
(23) Wood, L. L.; Cheng, S. S.; Edmiston, P. L.; Saavedra, S. S. *J. Am. Chem. Soc.* **1997**, *119*, 560.
(24) Edmiston, P. L.; Lee, J. E.; Cheng, S. S.; Saavedra, S. S.*J. Am. Chem. Soc.* **1997**, *119*, 571.
(25) Edmiston, P. L.; Saavedra, S. S. *Biophys. J.* **1998**, *74*, 999.
(26) Edmiston, P. L.; Saavedra, S. S. *J. Am. Chem. Soc.* **1998**, *120*, 1665.
(27) Du, Y. Z.; Saavedra, S. S. *Langmuir* **2003**, *19*, 6443.
(28) Edwards, A. M.; Zhang, K.; Nordgren, C. E.; Blasie, J. K. *Biophys. J.* **2000**, *79*, 3105.
(29) Kondo, A.; Oku, S.; Murakami, F.; Higashitani, K. *Colloids Surf., B* **1993**, *1*, 197.
(30) Welzel, P. B. *Thermochim. Acta* **2002**, *382*, 175.
(31) Burkett, S. L.; Read, M. J. *Langmuir* **2001**, *17*, 5059.
(32) Schwinte, P.; Ball, V.; Szalontai, B.; Haikel, Y.; Voegel, J. C.; Schaaf, P. *Biomacromolecules* **2002**, *3*, 1135.
(33) Wang, J.; Buck, S. M.; Chen, Z. *J. Phys. Chem. B* **2002**, *106*, 11666.
(34) Xia, N.; May, C. J.; McArthur, S. L.; Castner, D. G. *Langmuir* **2002**, *18*, 4090.
(35) Petralli-Mallow, T. P.; Plant, A. L.; Lewis, M. L.; Hicks, J. M. *Langmuir* **2000**, *16*, 5960.
(36) El Kasmi, A.; Leopold, M. C.; Galligan, R.; Robertson, R. T.; Saavedra, S. S.; El Kacemi, K., Bowden, E. F. *Electrochem. Commun.* **2002**, *4*, 177.
(37) Oberholzer, M. R.; Wagner, N. J.; Lenhoff, A. M. *J. Chem. Phys.* **1997**, *107*, 9157.
(38) Gray, J. J.; Bonnecaze, R. T. *J. Chem. Phys.* **2001**, *114*, 1366.
(39) Zhou, J.; Tsao, H. K.; Sheng, Y. J.; Jiang, S. Y. *J. Chem. Phys.* **2004**, *121*, 1050.
(40) Zhou, J.; Chen, S. F.; Jiang, S. Y. *Langmuir* **2003**, *19*, 3472.
(41) Chen, S. F.; Liu, L. Y.; Zhou, J.; Jiang, S. Y. *Langmuir* **2003**, *19*, 2859.
(42) Wang, H.; Castner, D. G.; Ratner, B. D.; Jiang, S. *Langmuir* **2004**, *20*, 1877.
(43) Juffer, A. H.; Argos, P.; DeVlieg, J. *J. Comput. Chem.* **1996**, *17*, 1783.
(44) Ravichandran, S.; Madura, J. D.; Talbot, J. *J. Phys. Chem. B* **2001**, *105*, 3610.
(45) Tobias, D. J.; Mar, W.; Blasie, J. K.; Klein, M. L. *Biophys. J.* **1996**, *71*, 2933.
(46) Nordgren, C. E.; Tobias, D. J.; Klein, M. L.; Blasie, J. K. *Biophys. J.* **2002**, *83*, 2906.
(47) Castells, V.; Yang, S. X.; van Tassel, P. R. *Phys. Rev. E* **2002**, *65*, 031912.
(48) Wong, C. F.; Zheng, C.; Shen, J.; McCammon, J. A.; Wolynes, P. G. *J. Phys. Chem.* **1993**, *97*, 3100
(49) Simonson, T.; Perahia, D. *J. Am. Chem. Soc.* **1995**, *117*, 7987.

(50) Prabhu, N. V.; Dalosto, S. D.; Sharp, K. A.; Wright, W. W.; Vanderkooi, J. M. *J. Phys. Chem. B* **2002**, *106*, 5561.
(51) Roth, C. M.; Lenhoff, A. M. *Langmuir* **1993**, *9*, 962.
(52) Johnson, C. A.; Wu, P.; Lenhoff A. M. *Langmuir* **1994**, *10*, 3705.
(53) Roth, C. M.; Lenhoff, A. M. *Langmuir* **1995**, *11*, 3500.
(54) Asthagiri, D.; Lenhoff, A. M. *Langmuir* **1997**, *13*, 6761.
(55) Roth, C. M.; Sader, J. E.; Lenhoff, A. M. *J. Colloid Interface Sci.* **1998**, *203*, 218.
(56) Satulovsky, J.; Carignano, M. A.; Szleifer, I. *Proc. Natl. Acad. Sci. U.S.A.* **2000**, *97*, 9037.
(57) Fang, F.; Szleifer, I. *Biophys. J.* **2001**, *80*, 2568.
(58) Mrksich, M.; Whitesides, G. M. *Annu. Rev. Biophys. Biomol. Struct.* **1996**, *25*, 55.
(59) Prime, K. L.; Whitesides, G. M. *Science* **1991**, *252*, 1164.
(60) Ostuni, E.; Yan, L.; Whitesides, G. M. *Colloids Surf., B* **1999**, *15*, 3.
(61) Ostuni, E.; Chapman, R. G.; Holmlin, R. E.; Takayama, S.; Whitesides, G. M. *Langmuir* **2001**, *17*, 5605.
(62) Chaki, N. K.; Vijayamohanan, K. *Biosens. Bioelectron.* **2002**, *17*, 1.
(63) Bushnell, G. W.; Louie, G. V.; Brayer, G. D. *J. Mol. Biol.* **1990**, *214*, 585.
(64) MacKerell, A. D., Jr.; Bashford, D.; Bellott, R. L.; Dunbrack, R. L., Jr.; Evanseck, J. D.; Field, M. J.; Fischer, S.; Gao, J.; Guo, H.; Ha, S.; Joseph-McCarthy, D.; Kuchnir, L.; Kuczera, K.; Lau, F. T. K.; Mattos, C.; Michnick, S.; Ngo, T.; Nguyen, D. T.; Prodhom, B.; Reiher, W. E., III.; Roux, B.; Schlenkrich, M.; Smith, J. C.; Stote, R.; Straub, J.; Watanabe, M.; Wiorkiewicz-Kuczera, J.; Yin, D.; Karplus, M. *J. Phys. Chem. B* **1998**, *102*, 3586.
(65) MacKerell A. D. Personal communication.
(66) Feller, S. E.; MacKerell, A. D. *J. Phys. Chem. B* **2000**, *104*, 7510.
(67) Jorgensen, W. L.; Chandrasekhar, J.; Madura, J. D.; Impey, R. W.; Klein, M. L. *J. Chem. Phys.* **1983**, *79*, 926.
(68) Beglov, D.; Roux, B. *J. Chem. Phys.* **1994**, *100*, 9050.
(69) Berendsen, H. J. C.; Postma, J. P. M.; van Gunsteren W. F.; Dinola A.; Haak J. R. *J. Chem. Phys.* **1984**, *81*, 3684.
(70) Andersen, H. C. *J. Comput. Phys.* **1983**, *52*, 24.
(71) Auerbach, D. J.; Paul, W.; Lutz, C.; Bakker, A. F.; Rudge, W. E.; Abraham, F. F. *J. Phys. Chem.* **1987**, *91*, 4881.
(72) Humphrey, W. F.; Dalke, A.; Schulten, K. *J. Mol. Graphics* **1996**, *14*, 33.
(73) Stocker, U.; Spiegel, K.; van Gunsteren, W. F. *J. Biomol. NMR* **2000**, *18*, 1.